

# Statistical noise enhances quantumness benefits in spin-network quantum reservoir computing

Youssef Kora and Christoph Simon

*Department of Physics and Astronomy, University of Calgary, Calgary, Alberta, Canada  
Institute for Quantum Science and Technology, University of Calgary, Calgary, Canada and  
Hotchkiss Brain Institute, University of Calgary, Calgary, Canada*

(Dated: April 28, 2025)

Quantum reservoir computing offers a promising approach to the utilization of complex quantum dynamics in machine learning. Statistical noise inevitably arises in real settings of quantum reservoir computing (QRC) due to the practical necessity of taking a small to moderate number of measurements. We investigate the effect of statistical noise in spin-network QRC on the possible performance benefits conferred by quantumness. As our measures of quantumness, we employ both quantum entanglement, which we quantify by the partial transpose of the density matrix, and coherence, which we quantify as the sum of the absolute values of the off-diagonal elements of the density matrix. We find that reservoirs which enjoy a finite degree of quantum entanglement and coherence are more stable against the adverse effects of statistical noise on performance compared to their unentangled, incoherent counterparts. Our results indicate that the potential benefit reservoir computers may derive from quantumness depends on the number of measurements used for training and testing, and may indeed be enhanced by statistical noise. These findings not only emphasize the importance of incorporating realistic noise models, but also suggest that the search for quantum advantage may be aided rather than impeded by the practical constraints of implementation within existing machines.

## I. INTRODUCTION

As we advance further into the information age, it is imperative that we should scale up our ability to interact with data of unprecedented complexity and volume. It is thus of increasingly critical importance to endow machines with the ability to understand, manipulate, and respond to sequential data inputs. A primary challenge in this arena arises in the form of the so-called von Neumann bottleneck, in which the physical division of processing and memory units constrains processing speed [1]. In stark contrast, biological systems manage dynamic, continuous information processing with vastly superior efficiency and remarkably low energy usage [2, 3].

Reservoir computing (RC) is as a paradigm that promises to empower our machines in the face of these challenges [4–6]. At the heart of it is the reservoir, a dynamical system of very high dimensionality, which receives incoming streams of data and naturally generates transient internal states endowed with fading memory and nonlinear processing capabilities. Such dynamical complexity lends itself well to machine learning tasks requiring a strong capacity for retaining prior inputs, such as speech recognition, stock market prediction, and autonomous motor control for robots [7]. Early implementations of RC used randomly connected artificial neural networks or spiking neural networks [8], while physical realizations have emerged across various platforms, such as photonics [9–13], phonons [14, 15], magnons [16–18], spintronics [19–21], and neuromorphic nanomaterials [22, 23].

Recent years have witnessed the rise of *quantum* reservoir computing (QRC), which seeks to employ within the framework of RC the unique properties of quantum

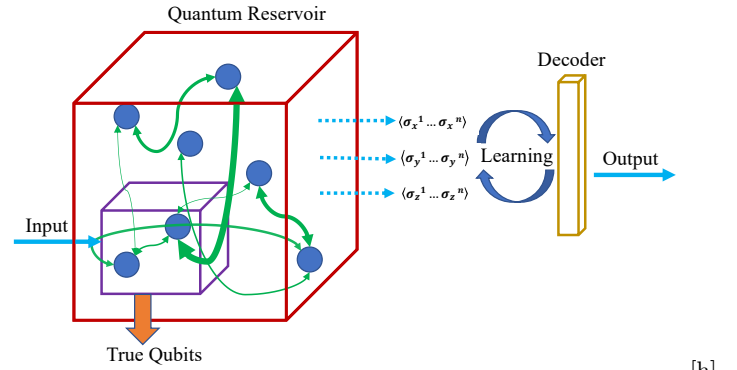


FIG. 1. **Schematic representation of spin-network quantum reservoir computing.** The reservoir (red box) comprises  $N$  qubits (blue spheres) with random and unchanging connections therebetween. At each timestep, the input data is injected into a fraction of the qubits, true qubits (purple box). Following injection, measurements are collected and sent to a classical decoder. The learning process is undertaken only by the classical connections between the reservoir and the decoder.

mechanics, such as quantum entanglement and coherence [24, 25]. One model of QRC utilizes networks of qubits [25–27], and another employs reservoirs comprising quantum-mechanical oscillators [28–30]. Here, we focus on the qubit-based approach, in which changes to qubit states are driven by sequential inputs that propagate through the reservoir’s quantum dynamics [31, 32]. Time-series data enters the system by injection into the so-called true nodes. The system, comprising both true nodes and hidden nodes, is allowed to evolve under the influence of the input. Finally, an output signal is read

from all nodes, to be used in the learning stage. Crucially, training only takes place at the output layer, which simplifies the learning considerably. A schematic of this general QRC mechanism is shown in Fig. 1.

The chief obstacle in the face of quantum computing and quantum machine learning is the decoherence inherent to the operation of the available quantum devices. Significant efforts have been dedicated to correcting or mitigating the resulting errors. However, there have been indications that, in certain scenarios, this dissipative noise may be harnessed to provide a computational benefit in the context of QRC [33–35]. Another recent observation of a potential slight enhancement of the performance of weakly-interacting spin-network QRC was attributed to dissipation [36].

There has also been a rising interest in understanding the potential advantage conferred by the essential aspects of quantum mechanics — quantum entanglement and superposition — in QRC. Such an advantage stands in contrast with the rather more traditional advantage of the exponential scaling of the state space, which can be present in the absence of quantumness [37]. Considerable research efforts have endeavored to investigate how quantumness might provide benefit to machine learning, in distributed learning over quantum networks [38], spin-network QRC [39], and oscillator-based QRC [40]. For example, Ref. 36, which sought to understand the physical circumstances conducing to an entanglement advantage in spin-network QRC, demonstrated that the presence of the entanglement advantage was, in the presence of dissipation, dependent on the frequency scale at which the input signal varies. This was interpreted as a consequence of the timescale introduced by dissipation, which determines whether quantum memory in the system can survive for long enough in the system for the input to manifest its temporal features, allowing the quantum reservoir computer to remember them.

Another important frontline in QRC is the ability to implement them on real machines. There are a number of candidate platforms which lend themselves well to the task, such as Rydberg atoms[41], superconducting qubits [42], photonics [13], and trapped ions [43]. Making contact with such implementations, however, faces a number of challenges, such as the necessity of contending with the measurement problem of quantum mechanics. Traditional QRC relies on projective measurements which destroy the quantum state, and thus require rewinding the system and input back in time every time a measurement is made. This, in combination with the necessity of repeating the process many times to compute quantum expectation values, leads to unfavorable time complexity and the need for an external memory. A number of approaches have been proposed to address this, such as those utilizing weak measurements [44], feedback protocols [45], an approach that combines the two [46], and artificial memory restriction [47]. However, it is generally the case that a real implementation will be rather severely constrained in the number of measurements that

can be practically extracted from the machine.

In this work, we seek to further understand the consequences of the statistical error introduced by the necessity of making a limited number of measurement in spin-network QRC, inspired by Ref. [48]. We are interested in understanding how this error interacts with the advantages that may be conferred by quantumness, which we measure by means of quantum entanglement and coherence. We find that the advantages potentially offered by quantumness are qualitatively dependent on the strength of this statistical noise; while having an overall adverse effect on performance, statistical noise is less detrimental to reservoir computers with higher amounts of quantum entanglement and coherence than reservoirs which are unentangled and incoherent. Our results not only highlight the importance of accounting for statistical noise in QRC simulations, but also demonstrate that the necessity to make fewer measurements may actually lead QRC systems to derive more benefit from quantumness. Indeed, the presence of this statistical noise was found to give rise to a quantumness benefit where there was none before.

The remainder of this paper is organized as follows: in section II we describe our dynamical models and methodology. We present and discuss our results in section III, and finally outline our conclusions in section IV.

## II. MODEL AND METHODOLOGY

### A. Physical System

Our quantum reservoir is a network of  $N = 4$  qubits obeying a generalized transverse-field Ising model [49, 50] with the Hamiltonian

$$\hat{H} = \sum_{i>j=1}^N J_{ij} \hat{\sigma}_i^x \hat{\sigma}_j^x + h \sum_{i=1}^N \hat{\sigma}_i^z, \quad (1)$$

where  $\hat{\sigma}_i^a$  ( $a = x, y, z$ ) are the Pauli operators,  $h$  is the transverse magnetic field, and  $J_{ij}$  are randomly generated network connectivities sampled from a uniform distribution in the interval  $[-J_s/2, J_s/2]$ . Ours is an open quantum system experiencing Markovian dynamics and obeying the Lindblad master equation

$$\frac{d\hat{\rho}}{dt} = \hat{\mathcal{L}}\hat{\rho} = -i[\hat{H}, \hat{\rho}] + \Gamma \sum_{i=1}^N \left( \hat{L}_i \hat{\rho} \hat{L}_i^\dagger - \frac{1}{2} \{ \hat{L}_i^\dagger \hat{L}_i, \hat{\rho} \} \right), \quad (2)$$

$\Gamma$  being the dissipation rate in this high-temperature decoherence channel [51], and  $\{\hat{L}_i\}$  are identifiable as the raising and lowering operators of the system. The unitary system experiences a dynamical phase transition between an ergodic phase and a many-body-localized phase determined by the ratio  $h/J_s$  [32].

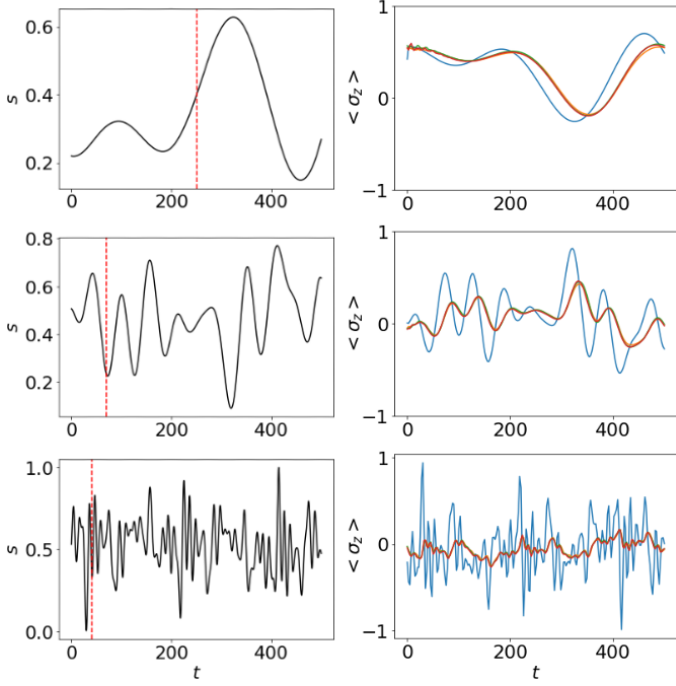


FIG. 2. (left) Examples of input sequences at three different frequency scales  $f = 0.2$  (top),  $f = 1$  (middle),  $f = 5$  (bottom). The red vertical dashed line corresponds to the maximum time delay at which the reservoir is successful in remembering past input. (right) The corresponding outputs of the reservoir at an interaction strength of  $J_s = 1$ , a transverse field of  $h = 2$ , an injection period of  $\Delta = 2.5$ , and a dissipation strength of  $\Gamma = 0.01$ . Blue corresponds to the input qubit.

### B. Input, Training, and Statistical Noise

We utilized input signals  $s_k$  with a frequency scale  $f$ , defined as the sum of 20 frequencies  $\{f_i\}$  chosen with equal linear spacing in the interval  $[f/5000, f/50]$ :

$$s_k = \sum_{i=1}^{20} \sin(2\pi f_i t_k + 2\pi\zeta), \quad (3)$$

where  $t_k$  is the time after  $k$  time steps, and  $\zeta$  is sampled from the uniform distribution in the interval  $[0, 1]$ . Input signals are normalized so as to lie between 0 and 1. The left panels of Fig. 2 show examples of these inputs, and the right panels show the corresponding outputs of the quantum reservoir at a representative choice of parameters.

The input signals are introduced into the quantum reservoir by means of reinitializing the state of one qubit that we call qubit 1, a commonly-used form of input injection [52]: we trace out the qubit in question and prepare it in the input-defined state  $|\psi_{s_k}\rangle = \sqrt{1-s_k}|0\rangle + \sqrt{s_k}|1\rangle$ , thereby transforming the quantum state of the system  $\rho$

into the product state

$$\hat{\rho} \rightarrow |\psi_{s_k}\rangle\langle\psi_{s_k}| \otimes \text{Tr}_1[\hat{\rho}]. \quad (4)$$

This injection occurs ever  $\Delta t = L\delta t$ , where  $L$  is the number of time steps between successive input injections, chosen so as to lie in the favorable range reported in Ref. [53] in the interest of rich dynamical behavior.

Our reservoirs are time-multiplexed; the outputs are extracted at time intervals of  $\Delta t/V$ , giving rise to  $NV$  virtual nodes. The readout signals are here restricted to  $\langle\sigma_z\rangle$ , and are trained in a linear regression to produce the desired function of the input, which in this work is the fundamental linear memory task [54]  $\bar{y}_k = s_{k-\tau}$  ( $\bar{y}_k$  being the target).

After training the system on multiple sequences, we test it using a different sequence of the same frequency scale  $f$ . We employ Tikhonov regularization in which a regularization parameter is chosen to maximize performance. The performance of the reservoir in a memory task with time delay  $\tau$  is called the memory capacity, which we compute as

$$C_{STM}^\tau = \frac{\text{cov}^2(y, \bar{y}^\tau)}{\sigma_y^2 \sigma_{\bar{y}^\tau}^2}, \quad (5)$$

where  $y$  is the output signal of the reservoir and  $\bar{y}^\tau$  is the target function at a time delay  $\tau$ .

The output signals of the reservoir, being a product of our simulations rather than real machines, are subject to a level of Gaussian statistical noise  $\sigma$  to simulate the necessity of taking a finite number of measurements when using a real machine as a quantum reservoir compute. The value of  $\sigma$ , whose effect on the physics is a primary subject of our investigation, corresponds to the number of measurements that would be made in a real setting. As in Ref. [48], the Gaussian standard deviation is taken to be inversely proportional to the square root of the number of measurements.

The quantum reservoir computer is characterized by the fading memory property [55], which guarantees that the memory capacity vanish at large  $\tau$ . Thus may the total memory capacity of the reservoir computer be defined as

$$C_{STM} = \sum_{\tau=0}^{\infty} C_{STM}^\tau. \quad (6)$$

### C. Entanglement and Coherence

We measure the amount of quantum entanglement in our reservoir computers by means of the logarithmic negativity [56, 57]

$$E_N(\rho) = \log_2 \|\rho^{\Gamma_A}\|_1, \quad (7)$$

where  $\|\cdot\|_1$  is the trace norm,  $\rho^{\Gamma_A}$  is the partial transpose with respect to subsystem A, and all possible bipartitions

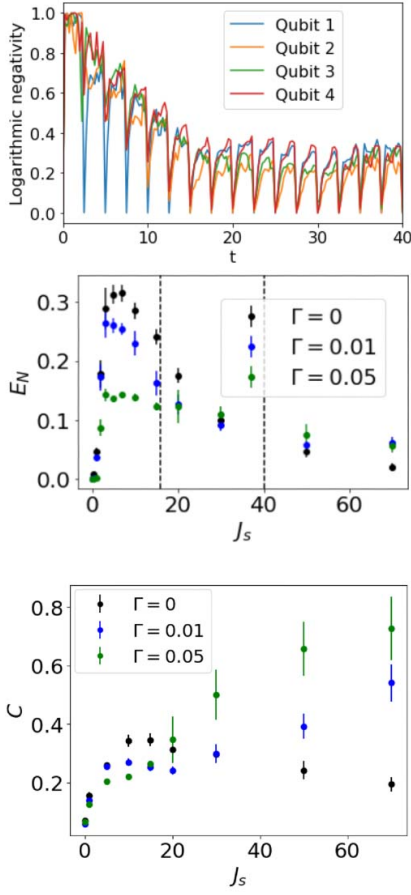


FIG. 3. (top) An example of the logarithmic negativity as a function of time - the entanglement abruptly drops whenever the input is injected. Each color corresponds to the bipartition in which the respective qubit labeled in the legend is isolated. (middle) Entanglement vs. interaction strength for the reservoir at a transverse field of  $h = 2$ , and an injection period of  $\Delta t = 2.5$ . The input of frequency of the signal is fixed at  $f = 0.2$  while the dissipation strength  $\Gamma$  is varied. (bottom) Coherence vs. interaction strength for the reservoir at the same physical conditions, at various dissipation strengths and constant frequency.

of the system are averaged over. Because of our mechanism of input injection, quantum entanglement abruptly plummets each time the input qubit (qubit 1) is reinitialized to reflect the input signal. This drop is naturally strongest for the entanglement corresponding to the bipartition isolating qubit 1. We show an example of this behaviour in Fig. 3 (top panel), where 4 different bipartitions are shown, each isolating one of the 4 qubits.

We quantify the coherence of a quantum state  $\rho$  by means of the  $l_1$ -norm of coherence [58, 59], which is given by

$$C = \sum_{i \neq j} |\rho_{ij}|, \quad (8)$$

and is normalized by its maximum value of  $2^N - 1$ .

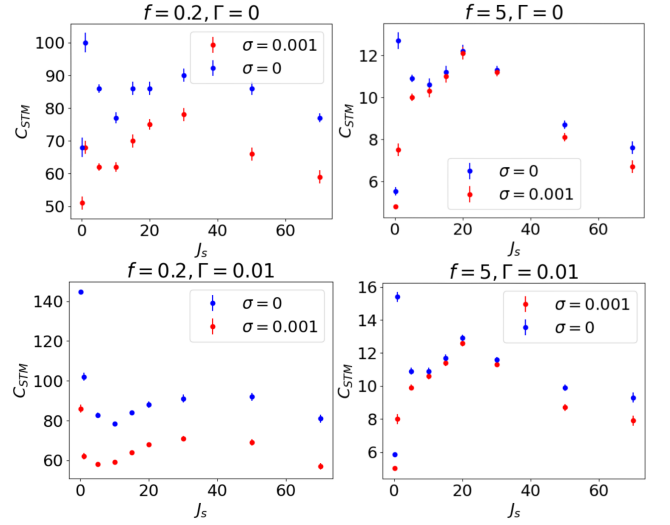


FIG. 4. The effect of the statistical noise level  $\sigma$  on the total memory capacity as a function of interaction strength, at two different dissipation strengths  $\Gamma$  and two input frequencies  $f$ . The transverse field is fixed at  $h = 2$ , and the injection period at  $\Delta t = 2.5$ .

### III. RESULTS AND DISCUSSION

We start by reviewing the behavior of the logarithmic negativity measure of entanglement. In Fig. 3 (middle panel), we present it as a function the interaction strength for a variety of dissipation strengths and input of frequencies, at a transverse field of  $h = 2$ , and an injection period of  $\Delta t = 2.5$ . The system undergoes a dynamical phase transition between an ergodic and many-body localized phase [32], marked by the region between the black, dashed lines. Entanglement peaks to the left of the transition, i.e., in the ergodic regime, and goes to zero at both extremes. It is also worth remarking that the peak is suppressed as  $\Gamma$  rises, but the frequency of the input signal has little to no effect.

To contrast, we examine the behavior of the coherence of our reservoirs in Fig. 3 (bottom panel). These results suggest that coherence exhibits a peak as a function of interaction strength only in the case of the isolated reservoir, whereas open systems gain coherence in the many-body localized phase. This behavior is consistent with Lindbladian many-body localization [60]. On the other hand, coherence appears to be insensitive to the frequency of the input, as is entanglement.

We now turn to the effect of Gaussian noise resulting from a finite number of measurements at the output layer. In Fig. 4, we compare the case without statistical noise with that subject to a statistical noise level of  $\sigma = 0.001$ , which corresponds to a million measurements. We look at conditions corresponding to both an entanglement advantage (high input frequency in the presence of finite dissipation) and an entanglement disadvantage (low input frequency in the presence of finite dissipation) [36].

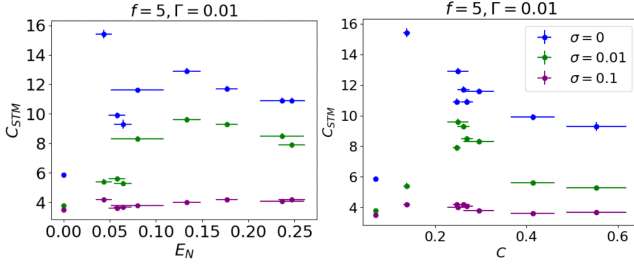


FIG. 5. The high-frequency case: The effect of the statistical noise level  $\sigma$  on the total memory capacity as a function of entanglement (left) and coherence (right). The dissipation strength is  $\Gamma = 0.01$ , and the input of frequency of the signal is  $f = 5$ . The transverse field is fixed at  $h = 2$ , and the injection period at  $\Delta t = 2.5$ .

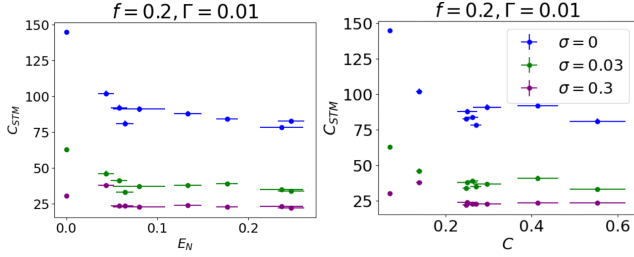


FIG. 6. The low-frequency case: The effect of the statistical noise level  $\sigma$  on the total memory capacity as a function of entanglement (left) and coherence (right). The dissipation strength is  $\Gamma = 0.01$ , and the input of frequency of the signal is  $f = 0.2$ . The transverse field is fixed at  $h = 2$ , and the injection period at  $\Delta t = 2.5$ .

Statistical noise invariably reduces performance, albeit to greatly varying extents. The low-frequency regime appears to generally sustain a greater performance reduction, both in the presence and absence of dissipation. The high-frequency regime, on the other hand, exhibits a performance loss only at the spike at low but non-zero interaction strength. This spike is present only in the absence of statistical noise, and is more pronounced in the presence of dissipation, as reported in Ref. 36. By considering only the case without statistical noise, one may be tempted to conclude that dissipation might offer a computational advantage in that regime. However, our results here, which show that such a performance improvement does not hold in the presence of statistical noise, corroborate the argument made in Ref. 48 respecting the necessity of accounting for statistical noise resulting from a finite number of measurements.

We now proceed to intensify the effect of statistical noise (which amounts to making fewer measurements), first in the high-frequency regime that decidedly benefits from quantum entanglement. Fig. 5 shows, for an input frequency of  $f = 5$  and a dissipation strength of  $\Gamma = 0.01$ , the total memory capacity for a wide range of statistical noise levels. Our most intense statistical noise level is  $\sigma = 0.3$ , which corresponds to roughly 10 measurements.

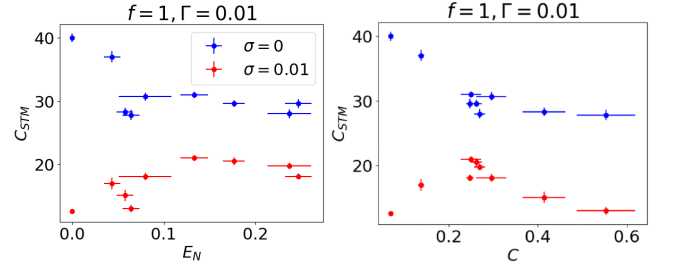


FIG. 7. The intermediate-frequency case: The effect of the statistical noise level  $\sigma$  on the total memory capacity as a function of entanglement (left) and coherence (right). The dissipation strength is  $\Gamma = 0.01$ , and the input of frequency of the signal is  $f = 1$ . The transverse field is fixed at  $h = 2$ , and the injection period at  $\Delta t = 2.5$ .

The memory capacity is invariably reduced by increasing the statistical noise, but the amount of performance loss is dependent on the amount of entanglement and coherence in the reservoir.

This observation raises an important question: what happens to the entanglement advantage as the rising statistical noise level causes the performance to drop? Our results in the left panel of Fig. 5 indicate that the entanglement advantage very much persists, notwithstanding the overall reduction in memory capacity. We also found it interesting to look at how performance behaves as a function of coherence rather than entanglement. These results are shown in the right panel of the same figure, and they tell a similar story, indicating that both entanglement and coherence can function as measures of quantumness whose presence may confer a computational advantage on reservoir computers. Specifically, there is a peak for both entanglement and coherence, but the peak is more pronounced as a function of coherence; this may be attributable to the continued growing of coherence in the localized regime. There seems to be an *excessive* amount of quantumness, as measured by either entanglement or coherence, that does not grant benefit. But since coherence continues to grow in the many-body localized phase while entanglement dies, as may be seen in Fig. 3, the performance peak is more defined with coherence on the x-axis.

A most interesting question presents itself at this point: what happens in the *low-frequency* (and finite dissipation) regime which does not appear to, in the absence of statistical noise, allow the system to derive much benefit from quantumness? In Fig. 6, we present our calculations of the total memory capacity for an input frequency of  $f = 0.2$  and a dissipation strength of  $\Gamma = 0.01$ . While ramping up the statistical noise unsurprisingly lowers performance throughout, it is clear from the figure that the high-entanglement, high-coherence reservoirs are more durable against the adverse effect of statistical noise. The points with low entanglement and coherence, on the other hand, are brought down the most as a function of statistical noise. Indeed, the negative trend in



the case without statistical errors does not persist as the number of measurements becomes of the order of 100, a peak having emerged at moderate levels of quantumness.

The behavior above evinces the possibility of turning an unfavorable trend into an unambiguously *positive* one. To further investigate this effect, we turn to the case of the intermediate input frequency of  $f = 1$ , whose results we present in Fig. 7. Remarkably, the quantum indifference (or slight disadvantage) observable without accounting for statistical noise does indeed turn into a distinctly favorable trend. At this level of statistical noise, reservoirs with finite quantum entanglement and coherence do perform better than the unentangled, incoherent reservoir. However, performance saturation appears more distinctly in the case of quantum entanglement on the x axis, whereas there seems to be rather a decline in the case of coherence, similar to the high-frequency case.

#### IV. CONCLUSIONS AND OUTLOOK

We studied the effect of statistical noise on the performance of a spin network QRC system in linear memory tasks, and its implications with respect to the frequency of the input signal, the presence of dissipation in the system, and quantumness as measured by quantum entanglement and coherence.

A more realistic model of statistical noise provides protection against possible spurious observations of performance enhancements due to, for instance, dissipation at low interaction strength. This emphasizes the importance of accounting for the reality of a finite number of measurements when employing real machines for QRC.

In general, performance is degraded by statistical noise resulting from a finite number of measurements. However, substantially quantum reservoirs are found to be more resistant to the effect of statistical noise than their non-quantum counterparts. As a result, it appears that, under the constraint of having to take a small to moderate number of measurements, we observe a quantum

benefit in certain regimes in which none was observed in the absence of statistical noise.

This quantumness was measured here by means of quantum entanglement and coherence. A moderate amount of either measure seems optimal under the conditions established as conducive to quantumness benefit, notwithstanding the continued growth of coherence into the many-body localized phase.

It is important to note that our model of statistical errors here does not lead to an uncertainty in the quantum state, for which we have an exact description by means of solving eq. 2. In a true experiment, however, the quantum state must be inferred from the measurements, and so the level of statistical noise would affect one's knowledge of the quantum state, and hence of the quantumness. In situations where quantumness cannot be measured to the desired precision, it is unclear whether its benefits may be meaningfully evaluated. The implications of statistical errors on the ability to accurately measure quantumness is a topic for future investigation.

Regardless of our choice of quantumness measure, we find that, within the limitation discussed above, statistical noise may elevate the system from a regime that does not benefit from quantumness to a regime that does. This suggests that constraints imposed by real implementations of QRC may, rather surprisingly, serve rather than obstruct the quest for the quantum advantage.

#### V. ACKNOWLEDGMENTS

This work was supported by the National Research Council through its Applied Quantum Computing Challenge Program, the Natural Sciences and Engineering Research Council (NSERC) of Canada through its NSERC Discovery Grant Program, the Alberta Major Innovation Fund, and Quantum City. We would also like to thank Khabat Heshami and Hadi Zadeh-Haghighi for the useful discussions and feedback.

- 
- [1] J. von Neumann. First draft of a report on the edvac. *IEEE Annals of the History of Computing*, 15(4):27–75, 1993.
  - [2] Chris Eliasmith, Terrence C. Stewart, Xuan Choo, Trevor Bekolay, Travis DeWolf, Yichuan Tang, and Daniel Rasmussen. A large-scale model of the functioning brain. *Science*, 338(6111):1202–1205, November 2012.
  - [3] Terrence C. Stewart, Trevor Bekolay, and Chris Eliasmith. Learning to select actions with spiking neurons in the basal ganglia. *Frontiers in Neuroscience*, 6, 2012.
  - [4] Herbert Jaeger and Harald Haas. Harnessing nonlinearity: Predicting chaotic systems and saving energy in wireless communication. *Science*, 304:78–80, 2004.
  - [5] Wolfgang Maass, Thomas Natschlager, and Henry Markram. Real-time computing without stable states: A new framework for neural computation based on perturbations. *Neural Computation*, 14(11):2531–2560, 2002.
  - [6] D. Verstraeten, B. Schrauwen, M. D’Haene, and D. Stroobandt. An experimental unification of reservoir computing methods. *Neural Networks*, 20:391–403, 2007.
  - [7] Gouhei Tanaka, Toshiyuki Yamane, Jean Benoit Heroux, Ryosho Nakane, Naoki Kanazawa, Seiji Takeda, Hidetoshi Numata, Daiju Nakano, and Akira Hirose. Recent advances in physical reservoir computing: A review. *Neural Networks*, 115:100–123, July 2019.
  - [8] Wilten Nicola and Claudia Clopath. Supervised learning in spiking neural networks with force training. *Nature Communications*, 8(1), December 2017.
  - [9] Kristof Vandoorne, Pauline Mechet, Thomas Van Vaerenbergh, Martin Fiers, Geert Morthier,

- David Verstraeten, Benjamin Schrauwen, Joni Dambre, and Peter Bienstman. Experimental demonstration of reservoir computing on a silicon photonics chip. *Nature Communications*, 5(1), March 2014.
- [10] Piotr Antonik, Marc Haelterman, and Serge Massar. Brain-inspired photonic signal processor for generating periodic patterns and emulating chaotic systems. *Physical Review Applied*, 7(5), May 2017.
- [11] Laurent Larger, Antonio Baylón-Fuentes, Romain Martinenghi, Vladimir S. Udaltsov, Yanne K. Chembo, and Maxime Jacquot. High-speed photonic reservoir computing using a time-delay-based architecture: Million words per second classification. *Physical Review X*, 7(1), February 2017.
- [12] Satoshi Sunada and Atsushi Uchida. Photonic neural field on a silicon chip: large-scale, high-speed neuro-inspired computing and sensing. *Optica*, 8(11):1388, November 2021.
- [13] Jorge García-Beni, Gian Luca Giorgi, Miguel C. Soriano, and Roberta Zambrini. Scalable photonic platform for real-time quantum reservoir computing. *Physical Review Applied*, 20(1), July 2023.
- [14] Guillaume Dion, Salim Mejaouri, and Julien Sylvestre. Reservoir computing with a single delay-coupled nonlinear mechanical oscillator. *Journal of Applied Physics*, 124(15), October 2018.
- [15] Claude Meffan, Taiki Ijima, Amit Banerjee, Jun Hirotani, and Toshiyuki Tsuchiya. Non-linear processing with a surface acoustic wave reservoir computer. *Microsystem Technologies*, 29(8):1197–1206, May 2023.
- [16] Adam Papp, Wolfgang Porod, and Gyorgy Csaba. Nanoscale neural network using non-linear spin-wave interference. *Nature Communications*, 12(1), November 2021.
- [17] Jack C. Gartside, Kilian D. Stenning, Alex Vanstone, Holly H. Holder, Daan M. Arroo, Troy Dion, Francesco Caravelli, Hidekazu Kurebayashi, and Will R. Branford. Reconfigurable training and reservoir computing in an artificial spin-vortex ice via spin-wave fingerprinting. *Nature Nanotechnology*, 17(5):460–469, May 2022.
- [18] Lukas Körber, Christopher Heins, Tobias Hula, Joo-Von Kim, Sonia Thlang, Helmut Schultheiss, Jürgen Fassbender, and Katrin Schultheiss. Pattern recognition in reciprocal space with a magnon-scattering reservoir. *Nature Communications*, 14(1), July 2023.
- [19] Jacob Torrejon, Mathieu Riou, Flavio Abreu Araujo, Sumito Tsunegi, Guru Khalsa, Damien Querlioz, Paolo Bortolotti, Vincent Cros, Kay Yakushiji, Akio Fukushima, Hitoshi Kubota, Shinji Yuasa, Mark D. Stiles, and Julie Grollier. Neuromorphic computing with nanoscale spintronic oscillators. *Nature*, 547(7664):428–431, July 2017.
- [20] Taishi Furuta, Keisuke Fujii, Kohei Nakajima, Sumito Tsunegi, Hitoshi Kubota, Yoshishige Suzuki, and Shinji Miwa. Macromagnetic simulation for reservoir computing utilizing spin dynamics in magnetic tunnel junctions. *Physical Review Applied*, 10(3), September 2018.
- [21] Sumito Tsunegi, Tomohiro Taniguchi, Shinji Miwa, Kohei Nakajima, Kay Yakushiji, Akio Fukushima, Shinji Yuasa, and Hitoshi Kubota. Evaluation of memory capacity of spin torque oscillator for recurrent neural networks. *Japanese Journal of Applied Physics*, 57(12):120307, October 2018.
- [22] Adam Z. Stieg, Audrius V. Avizienis, Henry O. Sillin, Cristina Martin-Olmos, Masakazu Aono, and James K. Gimzewski. Emergent criticality in complex turing b-type atomic switch networks. *Advanced Materials*, 24(2):286–293, October 2011.
- [23] Dmytro D. Yaremkevich, Alexey V. Scherbakov, Luke De Clerk, Serhii M. Kukhtaruk, Achim Nadzeyka, Richard Champion, Andrew W. Rushforth, Sergey Savel'ev, Alexander G. Balanov, and Manfred Bayer. On-chip phonon-magnon reservoir for neuromorphic computing. *Nature Communications*, 14(1), December 2023.
- [24] Keisuke Fujii and Kohei Nakajima. Harnessing disordered-ensemble quantum dynamics for machine learning. *Phys. Rev. Appl.*, 8:024030, Aug 2017.
- [25] K. Fujii and K. Nakajima. Quantum reservoir computing: A reservoir approach toward quantum machine learning on near-term quantum devices. In K. Nakajima and I. Fischer, editors, *Reservoir Computing*, Natural Computing Series. Springer, Singapore, 2021.
- [26] I. A. Luchnikov, S. V. Vintskevich, H. Ouerdane, and S. N. Filippov. Simulation complexity of open quantum dynamics: Connection with tensor networks. *Physical Review Letters*, 122(16), April 2019.
- [27] R. Martínez-Peña, J. Nokkala, G. L. Giorgi, R. Zambrini, and M. C. Soriano. Information processing capacity of spin-based quantum reservoir computing systems. *Cognitive Computation*, 15(5):1440–1451, October 2020.
- [28] L. C. G. Govia, G. J. Ribeill, G. E. Rowlands, H. K. Krovi, and T. A. Ohki. Quantum reservoir computing with a single nonlinear oscillator. *Physical Review Research*, 3(1), January 2021.
- [29] Johannes Nokkala, Rodrigo Martínez-Peña, Gian Luca Giorgi, Valentina Parigi, Miguel C. Soriano, and Roberta Zambrini. Gaussian states of continuous-variable quantum systems provide universal and versatile reservoir computing. *Communications Physics*, 4(1), March 2021.
- [30] Julien Dudas, Baptiste Carles, Erwan Plouet, Frank Alice Mizrahi, Julie Grollier, and Danijela Marković. Quantum reservoir computing implementation on coherently coupled quantum oscillators. *npj Quantum Information*, 9(1), July 2023.
- [31] Kohei Nakajima, Keisuke Fujii, Makoto Negoro, Kosuke Mitarai, and Masahiro Kitagawa. Boosting computational power through spatial multiplexing in quantum reservoir computing. *Physical Review Applied*, 11(3):034021–1, March 2019.
- [32] Rodrigo Martínez-Peña, Gian Luca Giorgi, Johannes Nokkala, Miguel C. Soriano, and Roberta Zambrini. Dynamical phase transitions in quantum reservoir computing. *Phys. Rev. Lett.*, 127:100502, Aug 2021.
- [33] Daniel Fry, Amol Deshmukh, Samuel Yen-Chi Chen, Vladimir Rastunkov, and Vanio Markov. Optimizing quantum noise-induced reservoir computing for nonlinear and chaotic time series prediction. *Scientific Reports*, 13(1), November 2023.
- [34] Yudai Suzuki, Qi Gao, Ken C. Pradel, Kenji Yasuoka, and Naoki Yamamoto. Natural quantum reservoir computing for temporal information processing. *Scientific Reports*, 12(1), January 2022.
- [35] L. Domingo, G. Carlo, and F. Borondo. Taking advantage of noise in quantum reservoir computing. *Scientific Reports*, 13(1), May 2023.
- [36] Youssef Kora, Hadi Zadeh-Haghighi, Terrance C Stewart, Khabat Heshami, and Christoph Simon. Frequency-and

- dissipation-dependent entanglement advantage in spin-network quantum reservoir computing, 2024.
- [37] Peter J. Ehlers, Hendra I. Nurdin, and Daniel Soh. Stochastic reservoir computers. *Nature Communications*, 16, March 2025.
  - [38] Dar Gilboa and Jarrod R. McClean. Exponential quantum communication advantage in distributed learning, 2023.
  - [39] Niclas Götting, Frederik Lohof, and Christopher Gies. Exploring quantumness in quantum reservoir computing. *Phys. Rev. A*, 108:052427, Nov 2023.
  - [40] Arsalan Motamedi, Hadi Zadeh-Haghighi, and Christoph Simon. Correlations between quantumness and learning performance in reservoir computing with a single oscillator, 2023.
  - [41] Rodrigo Araiza Bravo, Khadijeh Najafi, Xun Gao, and Susanne F. Yelin. Quantum reservoir computing using arrays of rydberg atoms. *PRX Quantum*, 3:030325, Aug 2022.
  - [42] Y. Suzuki, Q. Gao, K.C. Pradel, et al. Natural quantum reservoir computing for temporal information processing. *Scientific Reports*, 12:1353, 2022.
  - [43] H. Häffner, C.F. Roos, and R. Blatt. Quantum computing with trapped ions. *Physics Reports*, 469(4):155–203, 2008.
  - [44] Pere Mujal, Rodrigo Martínez-Peña, Gian Luca Giorgi, Miguel C. Soriano, and Roberta Zambrini. Time-series quantum reservoir computing with weak and projective measurements. *npj Quantum Information*, 9(1), February 2023.
  - [45] Kaito Kobayashi, Keisuke Fujii, and Naoki Yamamoto. Feedback-driven quantum reservoir computing for time-series analysis. *PRX Quantum*, 5(4):040325, November 2024.
  - [46] Tomoya Monomi, Wataru Setoyama, and Yoshihiko Hasegawa. Feedback-enhanced quantum reservoir computing with weak measurements. *arXiv preprint arXiv:2503.17939*, March 2025.
  - [47] Saud Ćindrak, Brecht Donvil, Kathy Lüdge, and Lina Jaurigue. Enhancing the performance of quantum reservoir computing and solving the time-complexity problem by artificial memory restriction. *Physical Review Research*, 6(1):013051, January 2024.
  - [48] Ana Palacios, Rodrigo Martínez-Peña, Miguel C. Soriano, Gian Luca Giorgi, and Roberta Zambrini. Role of coherence in many-body quantum reservoir computing. *Communications Physics*, 7(369), November 2024.
  - [49] R. B. Stinchcombe. Ising model in a transverse field. i. basic theory. *Journal of Physics C: Solid State Physics*, 6(15):2459, 1973.
  - [50] P. Pfeuty and R. J. Elliott. The ising model with a transverse field. ii. ground state properties. *Journal of Physics C: Solid State Physics*, 4:2370, 1971.
  - [51] H. Breuer and F. Petruccione. *The Theory of Open Quantum Systems*. Oxford University Press, Oxford, 2002.
  - [52] Pere Mujal, Johannes Nokkala, Rodrigo Martínez-Peña, Gian Luca Giorgi, Miguel C Soriano, and Roberta Zambrini. Analytical evidence of nonlinearity in qubits and continuous-variable quantum reservoir computing. *J. of Phys. Complex.*, 2(4):045008, 2021.
  - [53] R. Martínez-Peña, J. Nokkala, G. L. Giorgi, R. Zambrini, and M. C. Soriano. Information processing capacity of spin-based quantum reservoir computing systems. *Cognitive Computation*, 15:1440–1451, 2023.
  - [54] T. L. Carroll. Optimizing memory in reservoir computers. *Chaos*, 32:023123, 2022.
  - [55] Joni Dambre, David Verstraeten, Benjamin Schrauwen, and Serge Massar. Information processing capacity of dynamical systems. *Scientific Reports*, 2:514, 2012.
  - [56] G. Vidal and R. F. Werner. Computable measure of entanglement. *Phys. Rev. A*, 65:032314, Feb 2002.
  - [57] M. B. Plenio. Logarithmic negativity: A full entanglement monotone that is not convex. *Phys. Rev. Lett.*, 95:090503, Aug 2005.
  - [58] Alexander Streltsov, Gerardo Adesso, and Martin B. Plenio. Colloquium: Quantum coherence as a resource. *Reviews of Modern Physics*, 89(4):041003, October 2017.
  - [59] T. Baumgratz, M. Cramer, and M. B. Plenio. Quantifying coherence. *Physical Review Letters*, 113(14):140401, October 2014.
  - [60] Ryusuke Hamazaki, Masaya Nakagawa, Taiki Haga, and Masahito Ueda. Lindbladian many-body localization. *arXiv preprint arXiv:2206.02984*, June 2022.